LIQUEFACTION ANALYSIS OF SEAWALL STRUCTURES UNDER BOTH DRAINED AND UNDRAINED CONDITIONS

Jun WANG[1], Masayuk SATO[2], Nozomu YOSHIDA[3], Hiroki KUROSE[4] And Katsumi OZEKI[5]

SUMMARY

Two seawall structures damaged by soil liquefaction during past earthquakes, Showa Bridge site damaged during the 1964 Niigata earthquake and Uozaki-hama site during the 1995 Hyogoken-nambu earthquake, are analyzed by using the nonlinear effective stress dynamic response analysis code. The investigation are especially focused on the effect of drainage. The undrained analysis results in smaller displacement of quay wall compared with the analysis considering the seepage of excess porewater pressure. The investigation on excess porewater pressure and total stress indicate that undrained assumption has a tendency to suppress the displacement in order to keep the volume constant, and to overestimate horizontal load to quay wall.

INTRODUCTION

More than 30 years have passed after the 1964 Niigata and Alaskan earthquakes by which liquefaction was identified as one of the primary cause of damage to soil-structures and structures on the ground; the study of liquefaction has become an important research area in the earthquake geotechnical engineering. The most recent reminder of liquefaction and its destructive effect were the 1995 Hyogoken-Nambu earthquake during which severe damage was observed in the Kobe city and vicinity areas. Considerable effort has been devoted on the study of liquefaction during past 30 years, but the problems still remain very controversial on many aspects. Focusing on the numerical analysis field, one of the problems is drainage condition. Undrained assumption is frequently employed in the liquefaction analysis partly because duration of the earthquake is too short for excess porewater pressure to dissipate and partly because the analysis becomes simple. This assumption may be justified for the purpose to predict occurrence of liquefaction. In the case of liquefaction-induced flow, however, it is not justified because flow seems to continue even after the earthquake [Yoshida, 1998]. If drainage condition is important after the earthquake, it should also be effective during the earthquake as well, but it is not investigated at present.

In this study, response of two types of quay wall associated with liquefaction is examined under drained and undrained condition by nonlinear effective stress dynamic response analysis code STADAS-2. They are a sheet

1 *Tokyo Electric Power Services Co., Ltd.3-3,Higasi-Ueno 3-chome,Taito-ku,Tokyo 110,Japan Email: wang@aed.tepsco.co.jp*
2 *Tokyo Electric Power Services Co., Ltd.3-3,Higasi-Ueno 3-chome,Taito-ku,Tokyo 110,Japan Email: sato@aed.tepsco.co.jp*
3 *Engineering Research Institute, Sato Kogyo Co., Ltd, Tokyo, Japan Email: Nozomu.Yoshida@satokogyo.co.jp*
4 *Tokyo Electric Power Services Co., Ltd.3-3,Higasi-Ueno 3-chome,Taito-ku,Tokyo 110,Japan Email: kurose@aed.tepsco.co.jp*
5 *Tokyo Electric Power Services Co., Ltd.3-3,Higasi-Ueno 3-chome,Taito-ku,Tokyo 110,Japan Email: ozeki@aed.tepsco.co.jp*

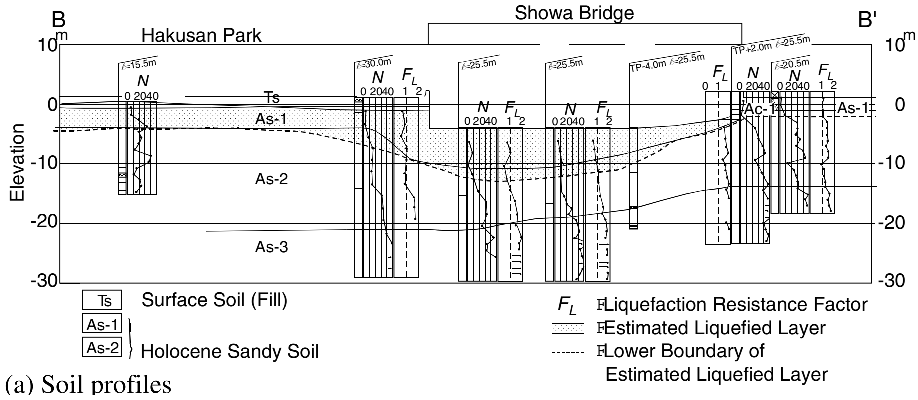

(a) Soil profiles

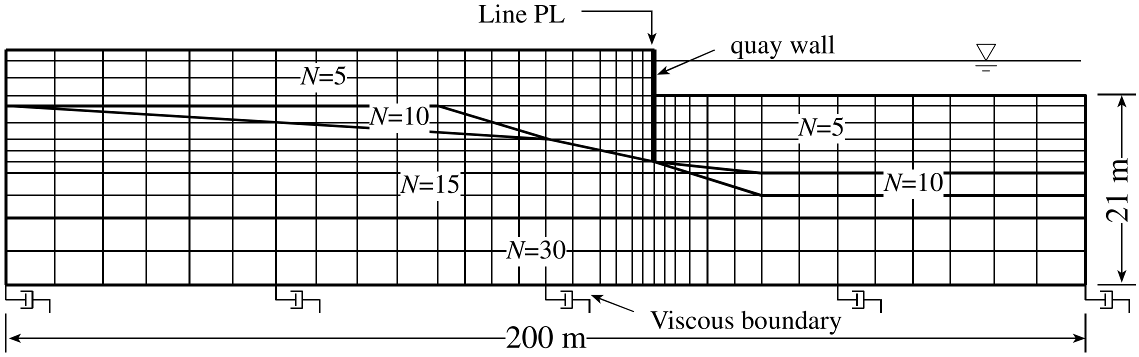

(b) FE mesh

Figure 1. Soil profiles and FE mesh at Syowa bridge site

Table 1. Physical properties of the sand

SPT N-value		5	10	15	30
Wet unit weight γ_t (gf/cm^3)		1.9	1.9	1.9	2.1
Shear modulus constant G_0 (kgf/cm^2)*		3.80×10^2	6.28×10^2	7.76×10^2	1.12×10^3
Reference confining pressure p_0 (kgf/cm^2) *		1.0	1.0	1.0	1.0
Shear modulus exponent m_G*		0.5	0.5	0.5	0.5
Bulk modulus constant B_0 (kgf/cm^2) *		5.07×10^2	8.38×10^2	1.03×10^3	1.49×10^3
Bulk modulus exponent m_B*		0.5	0.5	0.5	0.5
porosity n		0.4610	0.4186	0.4186	0.4060
Failure angle ϕ_f (deg.)		32.75	35.95	38.42	43.97
Angle at phase transform ϕ_p (deg.)		28.0	28.0	28.0	28.0
Permeability (cm/sec)	k_x	3.84×10^{-2}	1.92×10^{-2}	1.92×10^{-2}	1.92×10^{-2}
	k_y	3.84×10^{-2}	1.92×10^{-2}	1.92×10^{-2}	1.92×10^{-2}
Damping h (%)		3.0	3.0	3.0	3.0

*shear modulus $G = G_0\left(\frac{\sigma'_m}{p_0}\right)^{m_G}$, bulk modulus $K = B_0\left(\frac{\sigma'_m}{P_0}\right)^{m_B}$.

Table 2. Property of quay wall

Unit weight W (ton.f/m^3)	Young's modulus E (kgf/cm^2)	Shear modulus G (kgf/cm^2)	Sectional area A (m^2/m)	Second moment of inertia I (m^4/m)	damping h (%)
7.843	2.04×10^6	1.02×10^6	0.0153	8.745×10^{-5}	1.0

pile type quay walls at Syowa bridge site that was damaged during the 1964 Niigata earthquake and a caisson at Uozaki-hama site during the 1995 Hyogoken-nambu earthquake.

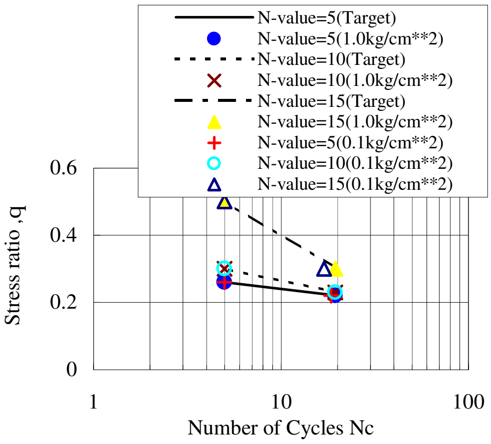

Figure 2. Comparison of liquefaction strength with initial confining pressure σ'=0.1 and 1.0kgf/cm^2

Table 3. The property of the joint element

K_n (kgf/cm)	K_s (kgf/cm)	Damping h (%)	Friction angle ϕ (deg.)
5.10×10^4	3.06×10^4	0.0	42.0

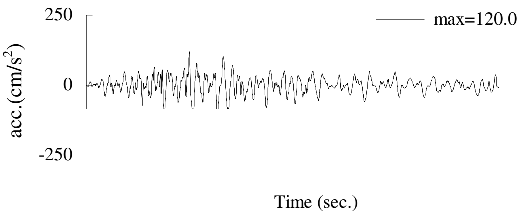

Figure 3. Input motion that are scaled from the record at Akita Prefecture office

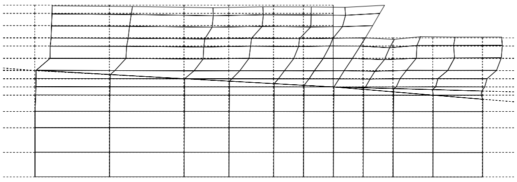

(a) undrained

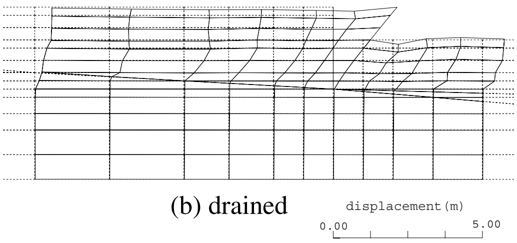

(b) drained

Figure 4. Deformation of the quay wall and surrounding regions at the end of analysis.

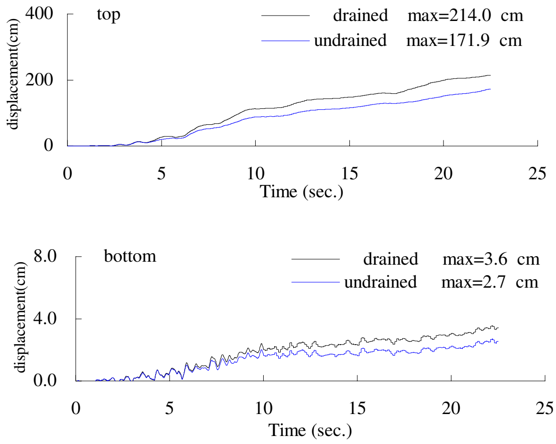

Figure 5. Horizontal displacement time histories at the top and the bottom of quay wall

2. RESULT OF ANALYSIS AND DISCUSSION

2.1 Syowa bridge site

(1) Model and method of analysis

Figure 1 shows soil profiles of the Showa Bridge site and its FE mesh. The subsoil is modeled into rectangular and triangle elements. The sheet pile quay walls are modeled into beam elements. The relative sliding and separation between the ground and quay wall is taken into account by the joint elements that considers water flow between the separation [Yoshida, 1993]. The hydrodynamic pressure acting along the riverside of the quay wall is considered by the added mass [Westergaard, 1933]. The viscous boundary [Joyner, 1975] is set at the bottom of the model in order to consider the effect of semi-infinite region beneath the ground. Physical properties of soil, quay wall and joint element are given in Tables 1, 2 and 3, respectively.

The modified Tobita-Yoshida Model [Ozeki et al., 1996] in employed for the constitutive model of sand. The model was originally proposed by Tobita and Yoshida [1994] based on elasto-plastic theory, and have been improved by the authors. The accuracy of the model, including effective stress path, stress-strain curve and liquefaction resistance curve, has been confirmed through various types of analysis such as sand foundation and reclaimed ground [Wang et al., 1998a; Sato et al, 1998; Wang et al., 1998b, Wang et al., 1999] as well as simulation of laboratory test.

Figure 2 compares the relationships between stress ratio $R = \tau/\sigma'_0$ and number of cycles to initial liquefaction obtained from the laboratory test and computed by using relevant parameters, in which initial liquefaction is

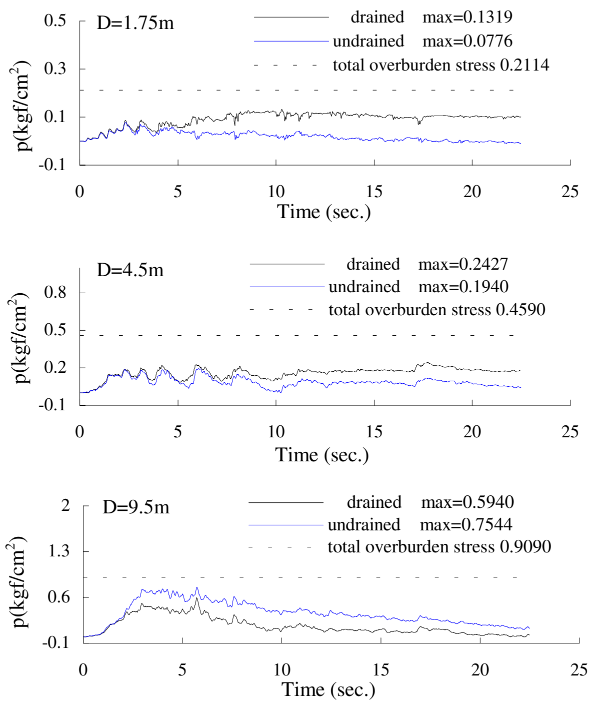

Figure 6. Excess porewater pressure time histories along the backfill side face of the quay wall

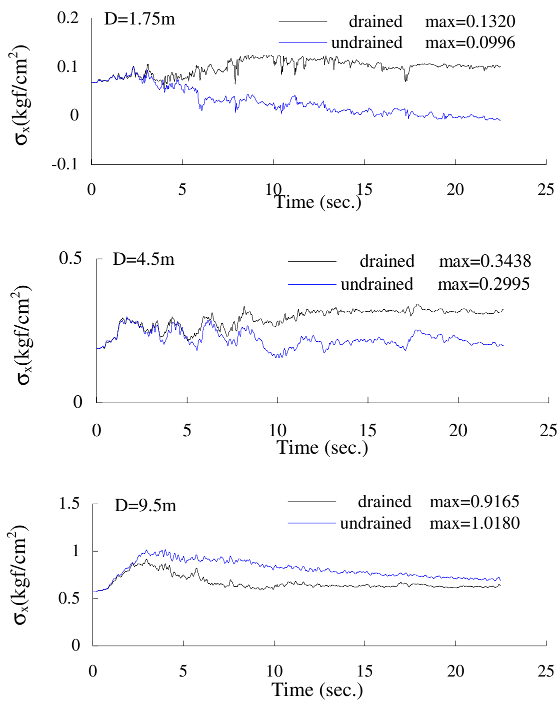

Figure 7. Horizontal total stress σ_x time histories along the backfill side face of the quay wall

defined when excess porewater reaches 95% of the initial effective confining stress. Here, τ denotes shear stress amplitude and ƒÐ is initial effective confining stress. It is seen that computed result agrees with target almost perfectly. It is also worth to note that computed liquefaction resistance (shear stress ratio) are nearly identical both under initial effective confining stresses of 1.0 kgf/cm^2 and 0.1 kgf/cm^2.

The acceleration recorded at the underground floor of the Akita Prefecture office at the time of the 1964 Niigata earthquake is used as input motion. The waves is scaled in time domain in order to adjust the predominant frequency considering the fault distance between the observed site and Showa Bridge site. The waveforms with peak acceleration of 120 cm/s^2 is shown in Figure 3.

Two types of analysis are conducted; the one allows drainage of excess porewater pressure and the other is under the undrained condition. The initial stresses are computed by the layer construction analysis using the same constitutive law.

(2) Results of analysis

Figure 4 compares the deformation of the quay wall and surrounding subsoil at the end of input motion, at 22.5 sec., and Figure 5 shows horizontal displacement time histories at the top and the bottom of the quay wall. It is clearly seen that displacement of the quay wall and deformation of the subsoil are greater in the drained case than those in the undrained case. The displacements at top and bottom of the quay wall at the end of analysis in the direction towards the river are 2.14m and 3.6cm, respectively, in the drained case, whereas they are 1.72m and 2.7cm, respectively, in the undrained case; the drained case produces more than 25 % larger displacement than the undrained case.

Because movement of the quay wall towards the river requires more volumetric strains in the sand elements adjacent to the quay wall than free field, excess porewater pressure is less generated in these regions compared with elements in free field. Actually, as shown in Figure 6, the excess porewater pressure along the backfill side face of the quay wall (Line PL in Figure 1) is much smaller than the total overburden stress in both drained and undrained cases. It is also noted that generated excess porewater pressure under the drained condition is higher than that under the undrained condition at 1.75 m depth, whereas excess porewater pressure at 9.5 m depth has the contrary tendency. This can be recognized by considering that, in the drained case, water flows towards the ground surface resulting in larger excess porewater pressure near the ground surface and smaller excess porewater pressure at deep depth. This water flow also results in larger horizontal total stress σ_x at GL-4.5 m depth than that under the undrained case. Especially, at 1.75m depth, σ_x becomes negative in the undrained

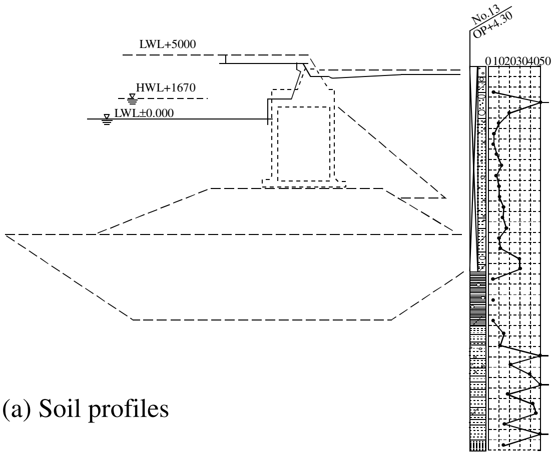

(a) Soil profiles

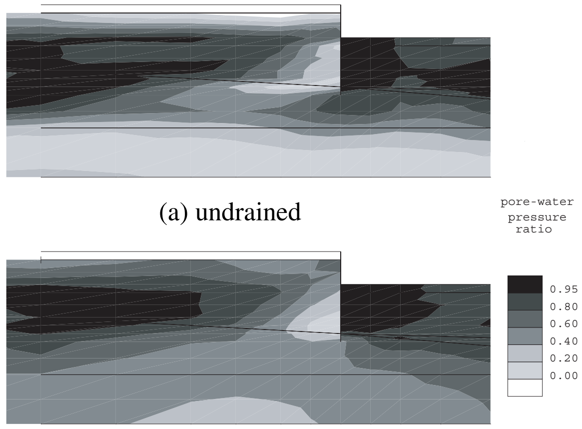

(b) drained

Figure 8. Excess porewater pressure distribution in the region near the quay wall at the end of analysis, at 22.5 sec.

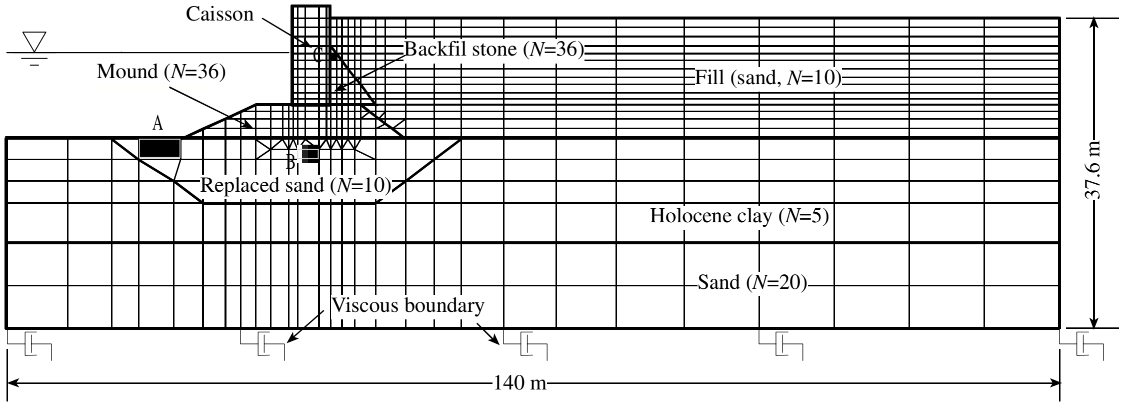

(b) FE mesh

Figure 9. Cross-section and FE mesh at Uozaki-hama site

case, which indicates that horizontal movement of quay wall is strongly suppressed. These behavior is the reason why analysis under drained condition gives larger horizontal displacement of quay wall.

Figure 8 shows excess porewater pressure distribution in the subsoil near the quay wall at the end of the analysis, at 22.5sec. The effect of the undrained condition discussed above is clearly seen in this figure; region where excess porewater pressure is small in backfill ground near the quay wall is greater in the undrained case than drained case. In addition, excess porewater pressures changes much smoothly in the drained case. This fact indicates that, although amount of water flow may be small during the earthquake, change in excess porewater pressure cannot be negligible because bulk modulus of water is large. In other words, undrained condition may not hold in the liquefaction analysis.

2.2 **Uozaki-hama site**

(1) Model

Figure 9 shows soil profiles in the backfill ground, movement of quay wall during the 1995 Hyogoken-nambu earthquake, and the FE mesh used in the analysis. The strategy to model the soil-structural system is same with previous analysis. The caisson and the ground are modeled into rectangular and triangle elements. The relative sliding and separation between the caisson and the ground are considered by the use of joint elements. The hydrodynamic pressure acting along the sea face of the caisson is taken into account by the added mass. Viscous boundary is used in order to consider the effect of semi-infinite region beneath the model. Physical properties and model parameters are shown in Tables 4 and 5. Figure 10 compares liquefaction strengths from the test with computed ones. Same as previous case, computed liquefaction strength agrees with test result well in a wide range of SPT N-value indicating the ability to express the liquefaction associated phenomena.

Table 4. The properties of the solid elements

Soil type		Holocene clay, N=5	Replaced sand, N=10	Sand, N=20	Mound and backfill crashed rock, N=36	Caisson
Wet unit weight γ_t (gf/cm^3)		1.5	1.9	1.85	2.07	2.22
Shear modulus constant G_0 (kgf/cm^2)*		4.00×10^1	6.28×10^2	1.700×10^3	3.27×10^2	9.06×10^4
Reference confining pressure p_0 (kgf/cm^2)*		1.0	1.0	1.0	1.0	—
Shear modulus exponent m_G*		0.5	0.5	0.5	0.5	—
Bulk modulus constant B_0 (kgf/cm^2)*		3.87×10^2	8.38×10^2	1.643×10^4	5.00×10^2	1.06×10^5
Bulk modulus exponent m_B*		0.5	0.5	0.5	0.5	—
porosity n		0.6667	0.4186	0.5080	0.3726	—
Failure angle ϕ_T (deg.)		31.9	35.92	38.03	75.18	—
Angle at phase transform ϕ_p (deg.)		28.0	28.0	28.0	28.0	—
Permeability (cm/sec)	k_x	3.4×10^{-5}	1.92×10^{-2}	3.4×10^{-5}	3.91×10^{-1}	—
	k_y	3.4×10^{-5}	1.92×10^{-2}	3.4×10^{-5}	3.91×10^{-1}	
Damping h (%)		3.0	3.0	3.0	3.0	3.0

*) : shear modulus $G = G_0\left(\frac{\sigma'_m}{p_0}\right)^{m_G}$, bulk modulus $K = B_0\left(\frac{\sigma'_m}{p_0}\right)^{m_B}$.

Table 5. The property of the joint element

Location	K_n (kgf/cm)	K_s (kgf/cm)	Damping h (%)	Friction angle ϕ (deg.)
Bottom of caisson	2.04×10^6	1.02×10^6	0.0	31.3
Ground side face	2.04×10^6	1.02×10^6	0.0	25.4
Interface between mound and fill	2.04×10^6	1.02×10^6	0.0	28.1

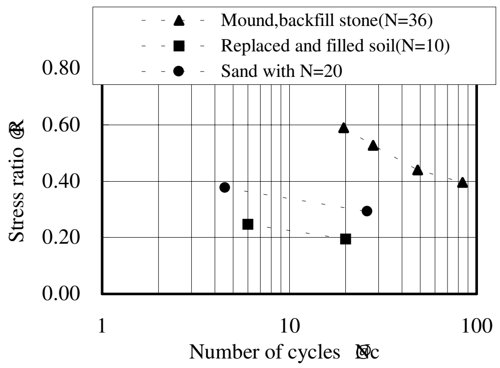

Figure 10. Comparison of liquefaction strength with initial confining pressure $\sigma' = 1.0$kgf/cm^2

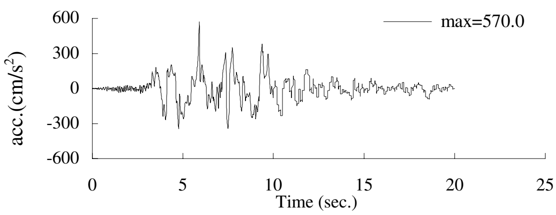

Figure 11. NS component of Port-Island accelerogram at GL=-16.4 m

The NS component of the Port-Island accelerogram at GL-16.4m recorded during the 1995 Hyogoken-nambu earthquake is used as input motion. The waveform with peak acceleration of 570 cm/s^2 is shown in Figure 11 The two cases, drained and undrained conditions, are analyzed. Initial stresses were computed by the layer construction analysis.

(2) Results

Figure 12 compares the deformations of the ground near the caisson at the end of the analysis, at 20.0 sec., and Figure 13 shows horizontal displacement time histories at the top and the bottom of the caisson. Caisson moves toward the sea and settle down in both analyses. Detailed investigation indicates that the caisson tilts slightly in the clockwise direction in the drained case, whereas small counter-clockwise rotation is observed in the undrained case. The displacements at the top and the bottom of the caisson are 1.07m and 1.04m, respectively, in the drained case. They are 0.89m and 0.98m in the undrained case. Again, the analysis considering seepage of excess porewater pressure produces larger displacement.

Figure 14 shows the distributions of the excess porewater pressure near the caisson at the end of the analysis, at 20.0 sec. Excess porewater pressures dissipate through the replaced sand, mound and back filling stone in the

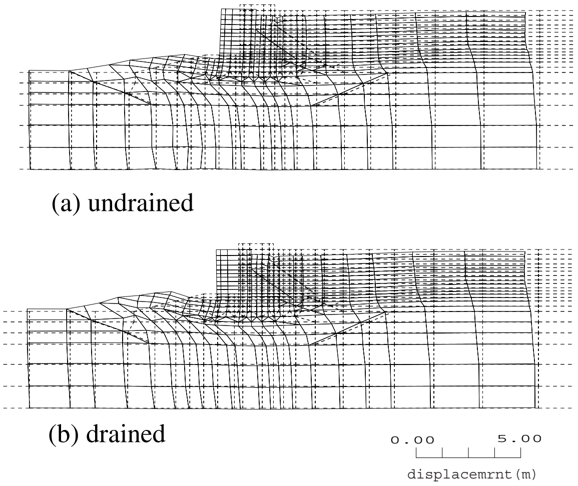

Figure 12. Deformation of the caisson and subsoil near it at 20.0sec.

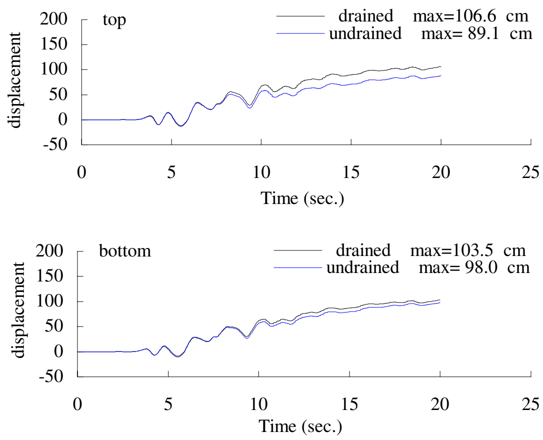

Figure 13. Horizontal displacement time histories at the top and the bottom of caisson

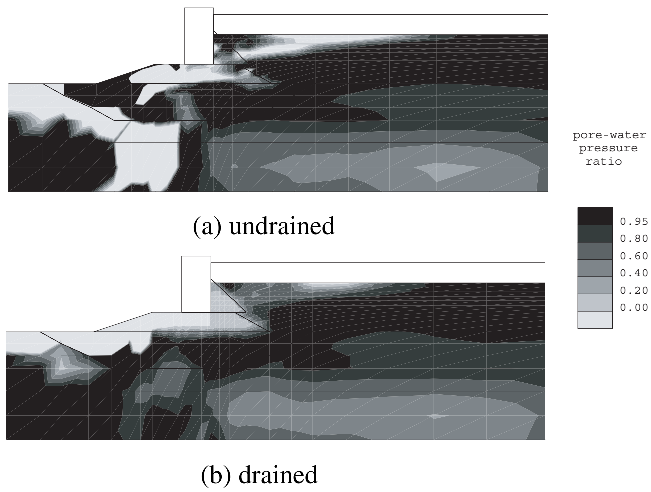

Figure 14. Excess porewater pressure distribution in the subsoil near the caisson at 20.0sec.

analysis considering the drainage because their permeability is much larger than the one of ordinary soil. On the other hand, in the undrained case, regions with high excess porewater pressure is observed near the ground surface, on the interface between replaced sand and mound, etc. The value of excess porewater pressure is nearly total overburden stress indicating the occurrence of complete liquefaction. Figures 15 and 16 illustrate the excess porewater pressure and the mean effective stress σ_m time histories of elements A, B and C among which elements A and B locates in the replaced sand and element C in the backfill stone region, respectively. For these elements, the excess porewater pressure becomes much higher in the undrained case than in the drained case so that the corresponding mean effective stresses (σ_m) become much smaller in the undrained case than in the drained case.

3. CONCLUDING REMARKS

Two seawall structures that are damaged during past earthquakes are analyzed by the nonlinear effective stress dynamic response analysis code under drained and undrained conditions. When focusing on the behavior of soils near the quay wall, behaviors computed under different drainage conditions are sometimes significantly different to each other, especially in displacements of the quay wall and the caisson, excess porewater pressure, and the stresses of the foundation ground. This indicates that undrained assumptions that are frequently used in the liquefaction analysis do not hold. It is important to consider the seepage of excess porewater pressure in order to predict the behavior of seawall structure precisely.

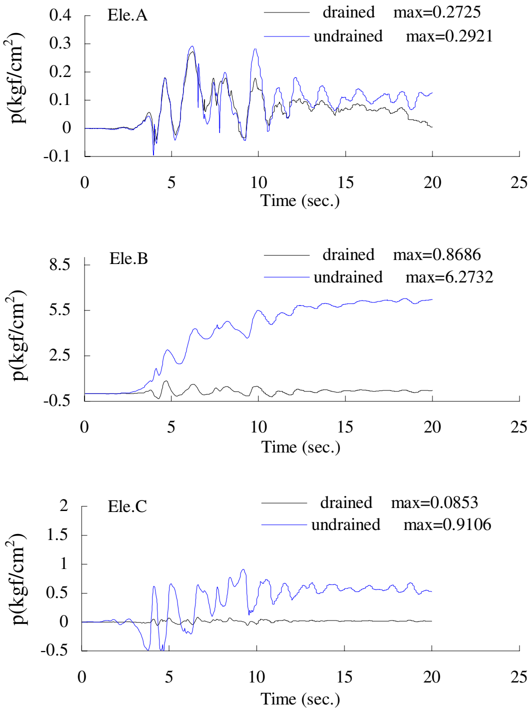

Figure15 Excess porewater pressure time histories of elements A, B and C, respectively

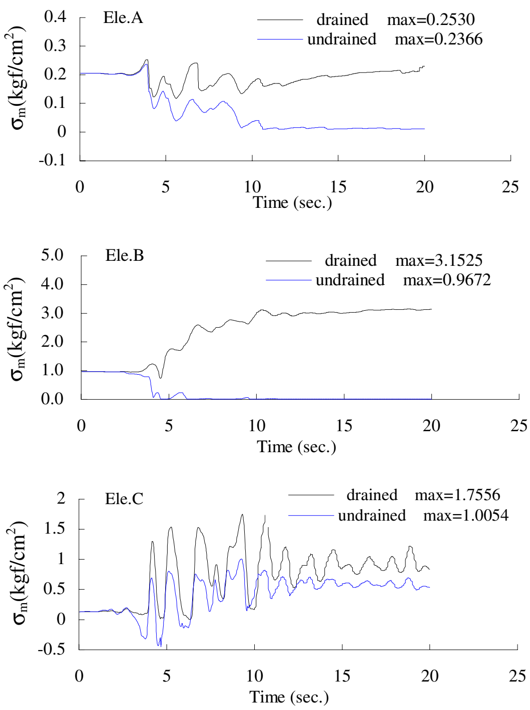

Figure16 Mean effective stress σ_m time history of elements A, B and C, respectively

4. REFERENCES

Joyner, W. B. (1975), "A method for calculating nonlinear response in two dimensions", *Bulletin of the Seismological Society of America*, 65-5, pp1337-1357

Ozeki, K., Wang, J., Kurose, H., Sato, M., Ishikawa, H. and Fujitani, M. (1996), "Simulation of the Laboratory Tests on Elements of Sand During Undrained Cycle Loading", *Proc. of the 51st Annual Conference of the Japan Society of Civil Engineering*, 3-(A), pp332-333. (in Japanese)

Sato, M., Wang, J. and Yoshida, N. (1998), "Effective Stress Analysis on the Damage to Sheet Pile(Phase 1: Influence of Micro-Vibration)", *Proc. of the 33rd Japan National Conference on Geotechnical Engineering, Yamaguchi*, 14-16 July, Vol.1, pp965-966. (in Japanese)

Tobita, Y. and Yoshida, N. (1994), "An isotropic bounding surface model for undrained cyclic behavior of sand: Limitation and Modification", *Proc., Int. Symp. on Pre-failure Deformation Characteristics of geomaterials*, Sapporo, pp457-462

Wang, J., Sato, M. and Yoshida, N. (1998a), "Effective Stress Analysis on the Damage to Sheet Pile(Phase 2: Influence of the Drained Condition)", *Proc. of the 33rd Japan National Conference on Geotechnical Engineering, Yamaguchi,* 14-16 July, Vol.1, pp967-968. (in Japanese)

Wang, J., Sato, M. and Yoshida, N. (1998b), "Effective Stress Analysis on the Damage to Sheet Pile at Showa Bridge Site During the 1964 Niigata Earthquake", *Proc. of the 53rd Annual Conference of the Japan Society of Civil Engineering*, Kobe, Oct., 3-(A), pp254-255. (in Japanese)

Wang, J., Kyono, T., Okuma, M. and Adachi, M. (1999), "Seismic Response of Offshore Thermal Power Plant with Soft-landing Foundation (Phase2: Effective Stress Analysis)", *Proc. of the 25th JSCE Earthquake Engineering Symposium*, July. (in Japanese)

Westergaard, H. M. (1933), "Water Pressures on Dams during Earthquakes", *Trans. ASCE*, 98, pp418-432

Yoshida, N. (1998), "Mechanism of liquefaction-induced flow", *Proc., Symposium on Flow and Permanent Displacement of Ground and Soil Structures during Earthquakes*, Japanese Geotechnical Society, pp53-70 (in Japanese)

Yoshida, N (1993), "A proposal of joint element for liquefaction analysis", *Proc. 22nd JSCE Earthquake Engineering Symposium-1993*, pp31-34